

KKH 22, the first dwarf spheroidal satellite of IC 342

Igor D. Karachentsev¹, Lidia N. Makarova¹, R. Brent Tully², Gagandeep S. Anand², Luca Rizzi³, Edward J. Shaya⁴,
and Viktor L. Afanasiev¹

¹ Special Astrophysical Observatory, the Russian Academy of Sciences, Nizhny Arkhyz, Karachai-Cherkessian Republic, Russia
369167

e-mail: ikar@sao.ru

² Institute for Astronomy, University of Hawaii, 2680 Woodlawn Drive, Honolulu, HI 96822, USA

³ W. M. Keck Observatory, 65-1120 Mamalahoa Hwy, Kamuela, HI 96743, USA

⁴ Astronomy Department, University of Maryland, College Park, MD 20743, USA

May 8, 2020

ABSTRACT

Aims. We present observations with the Advanced Camera for Surveys on the Hubble Space Telescope of the nearby dwarf spheroidal galaxy KKH 22 = LEDA 2807114 in the vicinity of the massive spiral galaxy IC 342.

Methods. We derived its distance of 3.12 ± 0.19 Mpc using the tip of red giant branch (TRGB) method. We also used the 6 m BTA spectroscopy to measure a heliocentric radial velocity of the globular cluster in KKH 22 to be $+30 \pm 10$ km s⁻¹.

Results. The dSph galaxy KKH 22 has the V-band absolute magnitude of $-12^m.19$ and the central surface brightness $\mu_{v,0} = 24.1^m/\square''$. Both the velocity and the distance of KKH 22 are consistent with the dSph galaxy being gravitationally bound to IC 342. Another nearby dIr galaxy, KKH 34, with a low heliocentric velocity of $+106$ km s⁻¹ has the TRGB distance of 7.28 ± 0.36 Mpc residing in the background with respect to the IC 342 group. KKH 34 has a surprisingly high negative peculiar velocity of -236 ± 26 km s⁻¹.

Key words. Galaxies: dwarf - Galaxies: distances and redshifts - Galaxies: individual: KKH 22 - Galaxies: photometry

1. Introduction

Nearby massive spiral galaxies with developed bulges (M 31, M 81, NGC 4258) have many dwarf satellites. In contrast, the number of dwarf satellites around spiral galaxies without apparent bulges (NGC 253, IC 342, M 101, NGC 6946) is relatively small. This circumstance was noted by Ruiz et al. (2015) and Javanmardi & Kroupa (2020). The situation becomes even clearer if we consider only dwarf spheroidal (dSph) satellites. Until recently, only one dSph companion, SC 22 = LEDA 3097727, was known around NGC 253. In recent years, Sand et al. (2014) and Toloba et al. (2016) discovered two new dSph satellites near NGC 253: Scl-MM-Dw1 and Scl-MM-Dw2. For a long time, only late-type dwarf satellites were known around M101. Now, Danieli et al. (2017), Karachentsev & Makarova (2019), and Bennet et al. (2019) have added the following four dSph satellites to them: M101-Dw A, M101-df 2, M101-df 3, and M101-Dw 9. However, no dSph satellites have been discovered around the massive late-type spirals IC 342, NGC 6946 or NGC 628.

IC 342 is the nearest massive late-type (Scd) spiral galaxy, which is situated in a zone of considerable extinction ($A_B = 2.02$ mag, Schlafly & Finkbeiner, 2011) at a distance of 3.28 Mpc (Saha et al. 2002). Its stellar mass corresponds to 10.60 dex in M_\odot , which is comparable with the stellar mass of the Milky Way (10.78 dex) and M 31 (10.73 dex), as well as the mass of NGC 253 (10.98 dex), M 101 (10.79 dex), and NGC 6946 (10.99 dex).

The first systematic attempt to search for dwarfs around IC 342 was undertaken by Borngen & Karachentseva (1985). The authors used photographic plates which were obtained with the wide-field Tautenburg 2 m telescope. Fifteen low surface brightness objects were found in the region of 40 square degrees

around IC 342. However, subsequent observations in the 21 cm line have shown that the radial velocities of these galaxies are in the range of 830 – 2500 km s⁻¹. Those candidate IC 342 satellites turned out to be background dwarf galaxies.

At present, there are nine galaxies for which the IC 342 is the most significant neighbour (the main disturber). All of them belong to late-type systems: Irr, Im, Sm, and Sd, which are listed in Section 5 (Table 2). Also, a dwarf irregular galaxy KKH 34 with a heliocentric velocity of $V_h = 105$ km s⁻¹ and an apparent magnitude of $B_T = 17.1$ mag, but with an uncertain distance estimate, has been a candidate as a remote companion to IC 342.

In this article, we report on measuring the distance and radial velocity of the galaxy KKH 22, which, by these parameters, has been revealed to be the first known dSph satellite of the IC 342. The object, KKH 34, that we observed turns out to be a background dwarf galaxy.

2. HST observations and TRGB distance

A northern (RA = 03:44:56.7, DEC = 72:03:52, J2000) low surface brightness galaxy KKH 22 (LEDA 2807114) was found by Karachentsev et al. (2001). It was not detected in the HI-line with the 100 m Effelsberg radio telescope at a level of 8 mJy. The galaxy is also undetected in the H α line with an upper limit of 5.7×10^{-16} erg cm⁻²s⁻¹ (Kaisin & Karachentsev 2013). These properties indicate it to be a dwarf spheroidal galaxy.

Observations of KKH 22 were performed with the Advanced Camera for Surveys (ACS) aboard the Hubble Space Telescope (HST) on October 14, 2019 as a part of SNAP project 15922 (PI R.B. Tully). Two exposures were made in a single orbit with the filters F606W (760 s) and F814W (760 s). The F814W image of

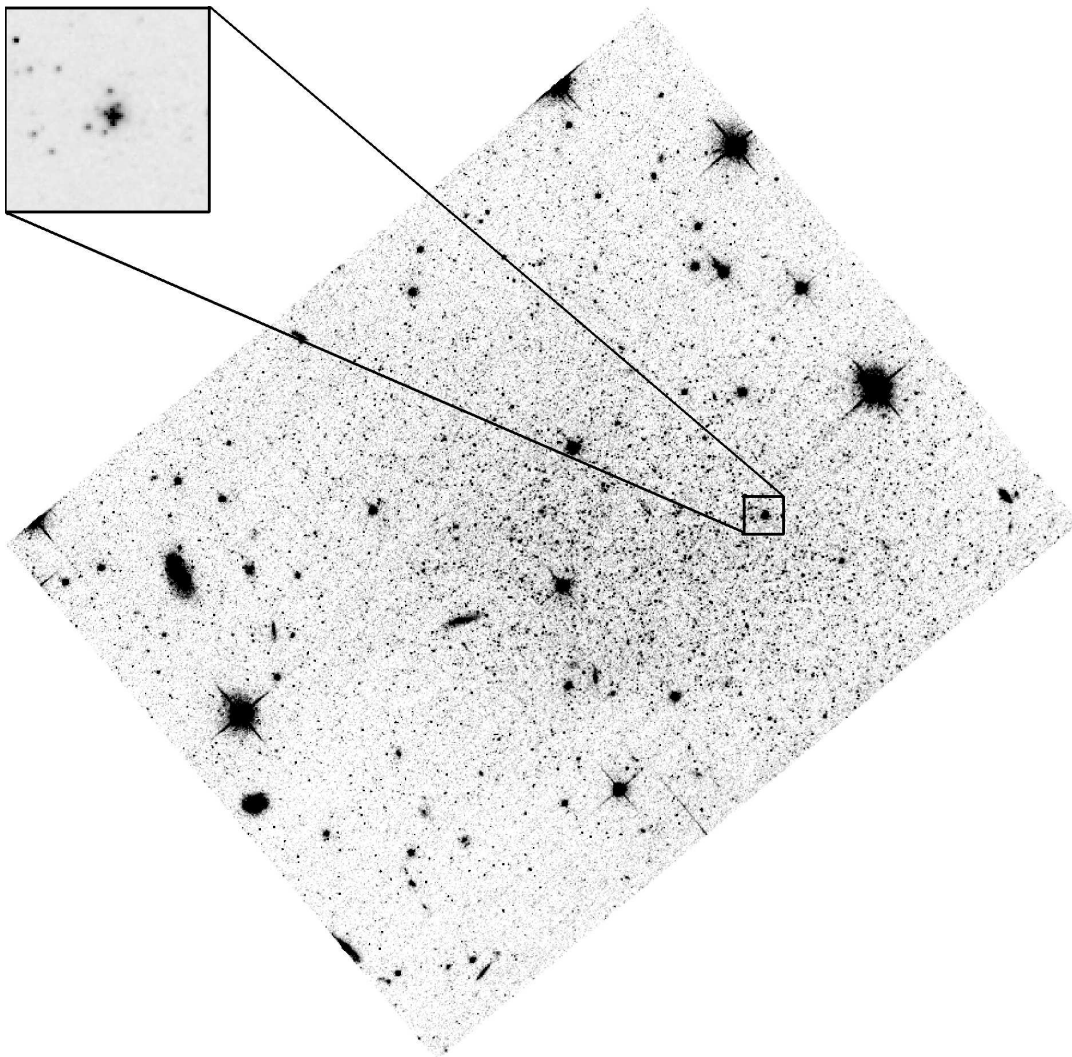


Fig. 1. HST/ACS image of KKH 22 through the F814W filter. The image size is 116 x 93 arcsec. North is up and east is left. The 5 arcsec region highlighted by the square is shown to contain a globular cluster.

the galaxy is presented in Fig.1. In the western part of KKH 22, which is highlighted by the $5'' \times 5''$ square, we found a globular cluster which is shown in the upper left side of Fig.1. Photometry of the cluster yields its total magnitude $V = 21.42$ and the colour $V - I = 0.86$ within the aperture $1''.4$.

We used the ACS module of the DOLPHOT package (<http://purcell.as.arizona.edu/dolphot/>) by Dolphin (2002) to perform photometry of resolved stars based on the recommended recipe and parameters. Only stars with good-quality photometry were included in the analysis. We selected the stars with a signal-to-noise ratio (S/N) of at least four in both filters, and with DOLPHOT parameters $crowd_{F606W} + crowd_{F814W} \leq 0.8$, $(sharp_{F606W} + sharp_{F814W})^2 \leq 0.075$. Artificial stars were inserted and recovered using the same reduction procedures to accurately estimate photometric errors. The resulting colour-magnitude diagram (CMD) in $F606W - F814W$ versus $F814W$ is plotted in Fig.2.

A maximum-likelihood method (Makarov et al. 2006) was applied to estimate the magnitude of the tip of the red giant branch (TRGB). We found $F814W(\text{TRGB})$ to be $23^m96 \pm 0^m13$. Following the zero-point calibration of the absolute magnitude of the TRGB developed by Rizzi et al. (2007), we obtained $M(\text{TRGB}) = -4.09$. Assuming $E(B - V) = 0.340$ from Schlafly

& Finkbeiner (2011) as for foreground reddening, we derived the true distance modulus of $(m - M)_0 = 27.47 \pm 0.13$ or the distance $D = 3.12 \pm 0.19$ Mpc.

3. Spectral observations

The globular cluster of KKH 22 was observed in the long-slit mode of the SCORPIO-2 focal reducer at the 6 m BTA telescope (Afanasiev & Moiseev 2011; Afanasiev et al. 2017), using the VPHG1200@860 grism as a disperser. The length of the slit was $6'$, while its width was $2''$. The spectral resolution was about 5 \AA . During our observations, we used the technique of subtracting the sky background using the 'nod-shuffle' method (Glasebrook & Bland-Hawthorn 2001). To do this, we obtained a series of exposures lasting 900 seconds in which the object was sequentially shifted along the slit by a gap of $+8''$ relative to the centre. A total of five pairs of such expositions were received. The average seeing was $1''.8$. The slit position, passing through several nearby foreground stars, is shown in Fig. 3.

The data reduction was carried out in a standard way using the IDL-based software package for reducing long-slit spectroscopic data obtained with SCORPIO-2. The data reduction included the following steps: bias subtraction, line curvature and

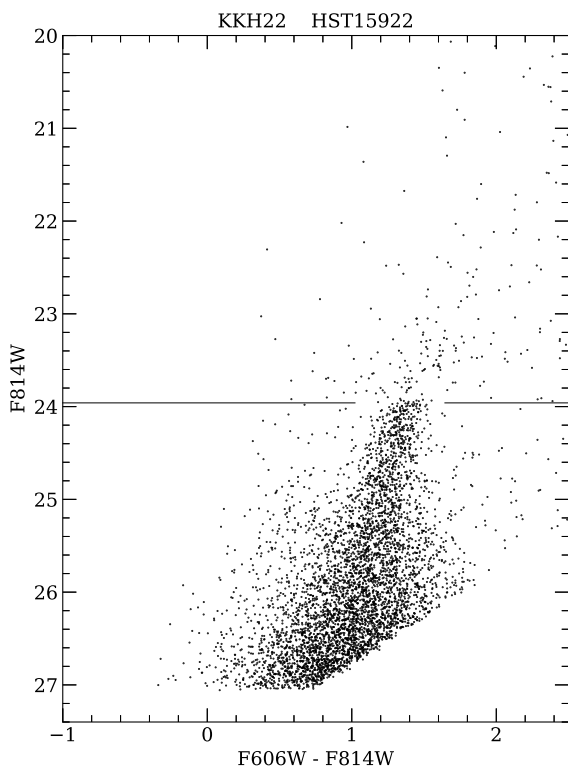


Fig. 2. Colour-magnitude diagram of KKH 22. The TRGB position is indicated by the horizontal line.

flat-field corrections, linearisation, and night sky subtraction. In the last step, unlike the standard one, the nod-shuffle algorithm was used. It consisted in the fact that two images were successively subtracted, in which the object was shifted by $16''$ along the slit. The result of this subtraction is shown in panel (C) of Figure 3. Then the five pairs of images obtained in this way were added together, and the resulting spectrum of the object and the reference star was obtained by integrating the image modularly in a $20''$ wide strobe along the slit (see left panel of Fig. 4)

Spectra of the target as well as of the reference star falling in the slit are shown in the left-hand panel of Fig. 4. Vertical lines indicate the positions of the calcium triplet lines: 8498\AA , 8542\AA , and 8662\AA . Using the cross-correlation method, we measured the observed radial velocity of $+36 \pm 10 \text{ km s}^{-1}$, which gives the heliocentric radial velocity of the globular cluster to be $+30 \text{ km s}^{-1}$. This velocity value is consistent with KKH 22 being gravitationally bound to IC 342, which has $V_{hel} = +29 \pm 1 \text{ km s}^{-1}$ (Crosthwaite et al. 2000).

4. Basic properties of KKH 22

In the Updated Nearby Galaxy Catalogue (UNGC, Karachentsev et al. 2013) KKH 22 was classified as a transition (Tr) type dwarf system. According to UNGC, the linear Holmberg’s diameter of the galaxy is 1.32 kpc, and the stellar mass is $(M_*/M_\odot) = 6.81$ dex at the measured distance of 3.12 Mpc. The absence of a noticeable flux from KKH 22 in the HI -line (Karachentsev et al. 2001) and in the $H\alpha$ line (Kaisin & Karachentsev 2013), as well as in the FUV-band indicates that the galaxy belongs to the class of spheroidal dwarfs with old stellar populations. The distribution of stars on the CM-diagram (Fig. 2) is concordant with this statement.

Some basic characteristics of the dwarf galaxy KKH 22 are presented in Table 1. We performed surface photometry of the

Table 1. Properties of KKH 22.

Parameter	Value
RA (J2000)	03:44:56.6
DEC (J2000)	+72:03:52
$(m - M)_o$, mag	27.47 ± 0.13
D , Mpc	3.12 ± 0.19
V_{hel} , km s^{-1}	30 ± 10
V_{LG} , km s^{-1}	251
$E(B - V)$	0.340
$E(V - I)$	0.477
V_0 , mag	15.28 ± 0.12
$(V - I)_o$	0.83 ± 0.09
$\mu_{V,0}$, mag/arcsec^{-2}	24.1 ± 0.2
$\mu_{I,0}$, mag/arcsec^{-2}	23.3 ± 0.2
$M(V)_0$	-12.19
A_{26} , kpc	1.32
axial ratio	0.52
$\log(M_*)$, M_\odot	6.81
$\log(M_{HI})$, M_\odot	< 6.34
$\log[SF(R_{HI})]$, M_\odot/yr	< -4.92
$\log[SF(R_{FUV})]$, M_\odot/yr	< -4.15
Globular cluster:	
RA (J2000)	03:44:50.49
DEC (J2000)	+72:03:56.4
V , mag	21.42 ± 0.03
$V - I$	0.86 ± 0.03
$M_{v,0}$, mag	-7.11
$(V - I)_0$	0.38

galaxy and determined its integrated magnitude $V = 16^m34 \pm 0^m12$ and colour index $V - I = 1.31 \pm 0.09$. Taking into account Galactic extinction (Schlafly & Finkbeiner 2011), the integrated apparent magnitude and integrated colour are $V_0 = 15^m28$ and $(V - I)_0 = 0.83$. The central surface brightness of the galaxy, $\mu_{v,0} = 24.1 \pm 0.2^m/\text{arcsec}^2$, and its absolute magnitude, $M_{v,0} = -12^m19$, are typical of dwarf spheroidal satellites around nearby massive spirals such as M 31 and M 81.

Figure 5 presents the distribution of the most luminous dSph satellites of the Milky Way (Fornax, Leo I, Sculptor, and Leo II), M 31 (NGC 147, And II, And I, CasSph, and PegSph), M 81 (KDG61, KDG64, KDG63, and F8D1), and NGC 253 (SC 22) according to their integrated absolute B-magnitudes and linear Holmberg’s diameters A_{26} , taken from UNGC. As one can see, the position of KKH 22 in this diagram, which is shown by an asterisk, does not stand out among other objects.

The last rows in Table 1 contain integral characteristics of the globular cluster. Given its absolute magnitude of $M_{v,0} = -7^m11$, the luminosity of the globular cluster contributes 1% of the total luminosity of the dwarf galaxy.

5. KKH 22 as a member of the IC 342 group

Judging by the distances and radial velocities of nearby galaxies, the gravitational dominance zone of IC 342 includes the nine dwarf satellites listed in Table 2. The table columns contain: (1) the galaxy name; (2,3) Galactic coordinates; (4,5) the angular and linear projected separation from IC 342; (6) the radial velocity of the expected satellite relative to IC 342; (7) the galaxy distance from the observer measured via the TRGB; and (8,9) a dimensionless ‘tidal index’ Θ_1 , indicating a density contrast which was contributed by the most significant neighbour

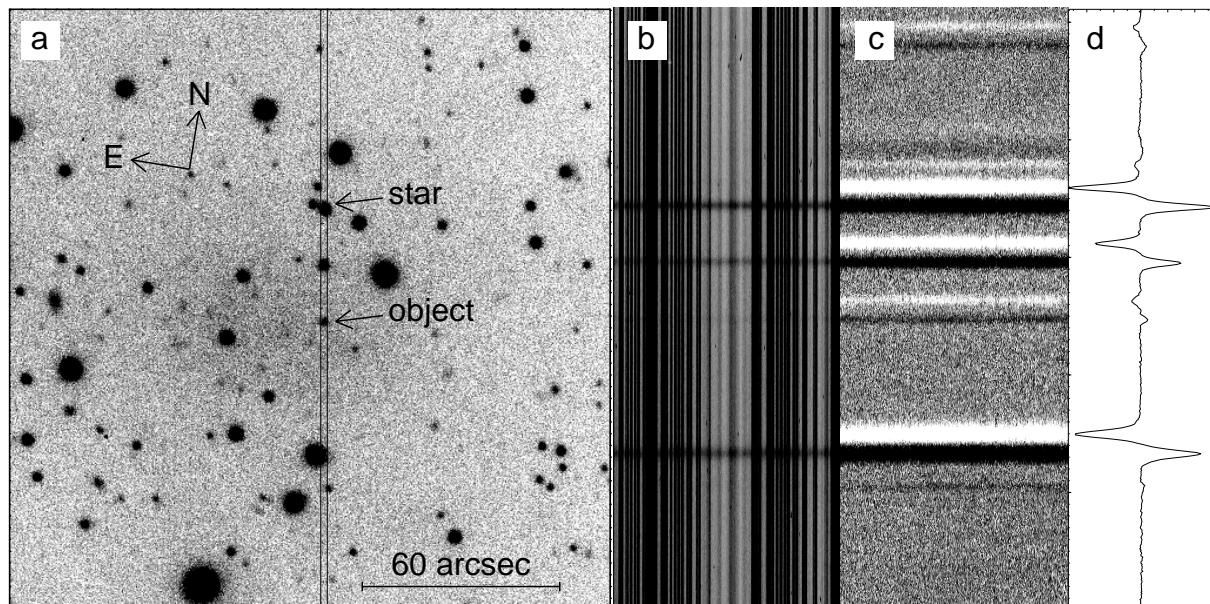


Fig. 3. Identification map and spectra of KKH22. (a) Localisation of the slit on the KH22 globular cluster, (b) the raw spectrum in the area of the infrared calcium triplet without subtracting the sky background, (c) the result of subtracting the sky background by the nod-shuffle procedure, and (d) the cross-section 2D spectra along the slit after the sky subtraction.

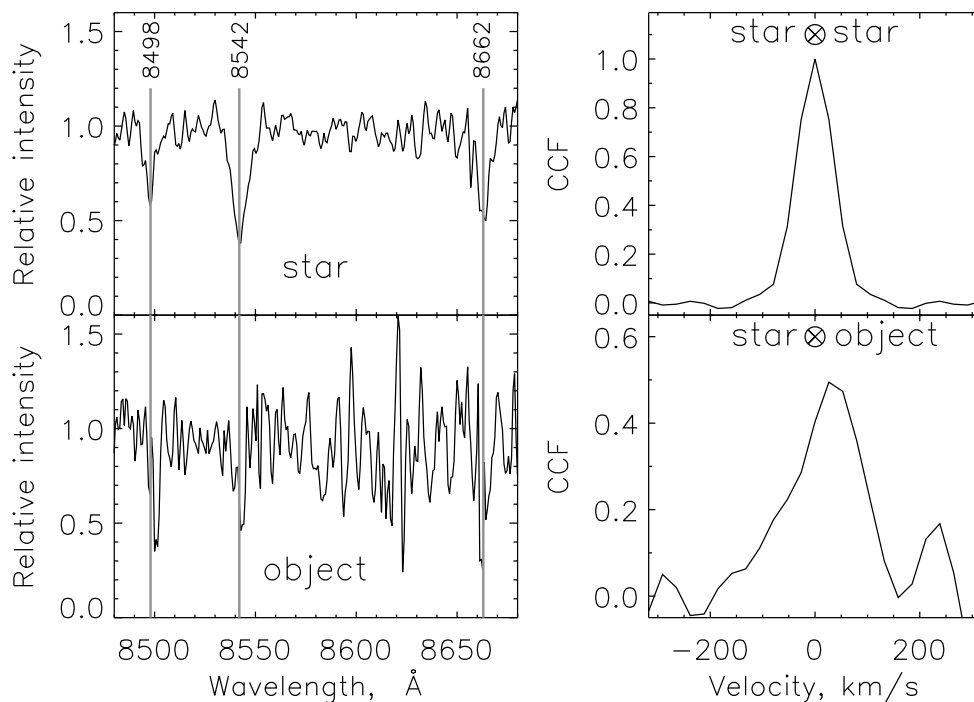


Fig. 4. Spectra showing the calcium triplet 8498/8542/8662Å lines for the globular cluster and for the neighbouring foreground star (left-hand panel) and cross-correlation functions showing that the observed radial velocity of the object is 36 ± 10 km/s (right-hand panel).

(‘main disturber’) of the galaxy as well as the main disturber’s name. The cases with positive Θ_1 can be considered as objects bound to the main disturber. As seen, all nine dwarfs, besides KKH 34, are gravitationally linked to IC 342. An updated version of the UNGC (<http://www.sao.ru/lv/lvgdb>) contains links to the sources of the data that are used.

The average distance of the expected satellites from the observer is 3.23 ± 0.09 Mpc, which practically coincides with the distance of the principal galaxy IC 342. The average radial veloc-

ity difference of the identified satellites, -49 ± 25 km s⁻¹, shows a weak asymmetry towards low radial velocities for the satellites. The distribution of galaxies in the IC 342 group in Galactic coordinates is characterised by significant asymmetry, with almost all of the dwarf companions residing at higher Galactic latitudes than IC 342. Such an eccentricity of the IC 342 position can be attributed to the substantial extinction in the Zone of Avoidance. Satellites within the influence of IC 342 that are closer to the Galactic plane may be hidden by obscuration. The search for

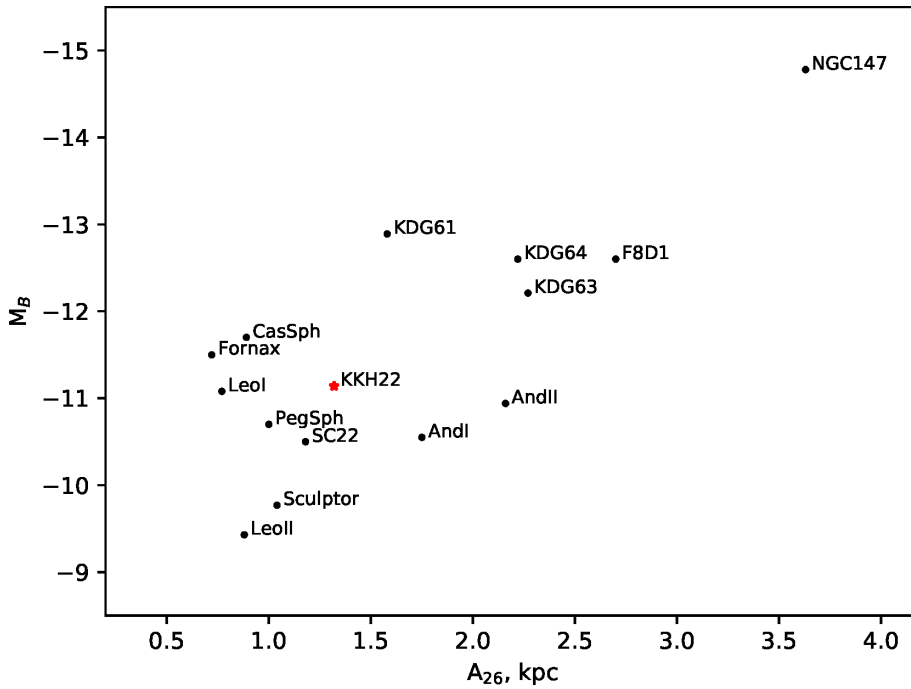


Fig. 5. Distribution of the most luminous dSph satellites of the Milky Way (Fornax, Leo I, Sculptor, and Leo II), M 31 (NGC 147, And II, And I, CasSph, and PegSph), M 81 (KDG61, KDG64, KDG63, and F8D1), and NGC 253 (SC 22) according to their integrated absolute B-magnitude and the linear Holmberg's diameter A_{26} .

Table 2. Known satellites of IC342.

Galaxy	l deg	b deg	r_p deg	R_p kpc	ΔV km s ⁻¹	D Mpc	Θ_1	Main disturber
IC342	138.17	10.58	0.00	0	0±1	3.28±0.30	-0.1	NGC 1569
KK35	138.20	10.31	0.27	16	-95±3	3.16±0.32	2.4	IC 342
UGCA86	139.76	10.65	1.59	91	36±5	2.98±0.28	1.1	IC 342
KKH22	135.50	13.57	4.01	229	7±10	3.12±0.19	1.6	IC 342
NGC1560	138.37	16.02	5.44	312	-74±1	2.99±0.21	0.8	IC 342
NGC1569	143.68	11.24	5.55	318	-138±3	3.19±0.10	1.1	IC 342
Cam A	137.25	16.20	5.69	326	-88±2	3.56±0.23	0.7	IC 342
Cam B	143.38	14.42	6.47	370	23±2	3.50±0.28	0.7	IC 342
UGA92	144.71	10.52	6.54	374	-151±2	3.22±0.11	1.8	NGC 1569
UGCA105	148.52	13.66	10.80	618	37±5	3.39±0.35	0.3	IC 342
KKH34	140.42	22.35	11.98	687	51±2	7.28±0.36	-0.6	Maffei 2

such objects by their emission in the 21 cm line is a difficult task since their radial velocities fall within the velocity range of the local Galactic hydrogen.

The only dSph satellite, KKH 22 (at $b = 13.6$ and with $A_B = 1.7$), is at a projected separation of 229 kpc from IC 342. Dwarf spheroidal companions to the Milky Way, Leo I and Leo II, have approximately the same spatial separations (250 kpc and 210 kpc). These values are all close to the virial radii of IC 342 and the Milky Way.

6. KKH 34

At a higher Galactic latitude, there is a dwarf irregular galaxy KKH 34= PGC 095594, with a radial velocity close to the IC 342 velocity. Based on a shallow CM-diagram, Karachentsev et al. (2003) determined the galaxy distance to be 4.61 Mpc. Since this distance estimation was considered to be unreliable, KKH 34 was included in our ongoing SNAP survey. An I -band image from a new ACS observation is shown in the upper

panel of Fig.6. The red giant branch with a TRGB position of $I_{TRGB} = 25^m60$ is visible in the corresponding colour-magnitude diagram (bottom panel of Fig.6). Taking the Galactic extinction of $A_I = 0^m361$ into account, we obtain $(m-M)_0 = 29.31 \pm 0.11$ or $D = 7.28 \pm 0.36$ Mpc for the galaxy distance module. Parameters for this galaxy are presented in the last row of Table 2.

At this revised distance, KKH 34 is 4 Mpc behind the IC 342 group, but only 2 Mpc from the Maffei group (Anand et al. 2019a). At the radial velocity of KKH 34 relative to the Local Group centroid of $V_{LG} = 295$ km s⁻¹ (Begum et al. 2008) and an assumed Hubble parameter of 73 km s⁻¹ Mpc⁻¹, the peculiar velocity of this galaxy is -236 ± 26 km s⁻¹. This motion towards us has the same sign but is greater than the -128 ± 33 km s⁻¹ of the Maffei group, which was reported by Anand et al. The study of the Local Void from Tully et al. (2019) provides an explanation for these motions. The Local Void is generating a currently well-documented displacement of the Local Sheet (Anand et al. 2019b) towards the negative supergalactic pole (towards nega-

tive SGZ). With a realisation of the full extent of the Local Void, it becomes apparent that the Local Void not only dominates at positive SGZ in our proximity but also at positive SGX in the space between us and the Perseus-Pisces filament (Haynes & Giovanelli 1986). The Maffei group and KKH 34 somewhat further back are experiencing the push of this void.

7. Concluding remark

In the Introduction, we address the fact that luminous bulgeless galaxies suffer from a lack of dwarf spheroidal satellites. Recently, Karachentsev & Karachentseva (2019) noted another feature of nearby massive Sc-Sd galaxies. Their mean estimate of total mass via the orbital motions of small companions, taken in relation to the stellar mass, is $\langle M_{orb}/M_* \rangle = 22 \pm 5$. This quantity is two times and four times less than the mean ratios for Sab-Sbc and for E, S0, and Sa galaxies, respectively. It is quite possible that both of these features of the bulgeless galaxies have a common evolutionary cause.

Acknowledgements. This work is based on observations made with the NASA/ESA Hubble Space Telescope and the 6 metre BTA telescope. STScI is operated by the Association of Universities for Research in Astronomy, Inc. under NASA contract NAS 5–26555. The work in Russia is supported by RFBR grant 18–02–00005.

REFERENCES

- Afanasiev, V.L., Amirkhanian, V.R., Moiseev, A.V., et al. 2017, *AstrBu*, 72, 458
- Afanasiev, V., & Moiseev, A. 2011, *Baltic Astronomy*, 20, 363
- Anand, G.S., Tully, R.B., Rizzi, L., et al. 2019a, *ApJ*, 872, L4
- Anand, G.S., Tully, R.B., Rizzi, L., et al. 2019b, *ApJ*, 880, 52
- Begum, A., Chengalur, J.N., Karachentsev, I.D., et al. 2008, *MNRAS*, 386, 1667
- Bennet, P., Sand, D.J., Crnoevic, D., et al. 2019, *ApJ*, 885, 153
- Borngen, F., & Karachentseva, V.E., 1985, *Astron.Nachr*, 306, 301
- Crosthwaite, L.P., Turner, J.L., & Ho, P.T.P., 2000, *AJ*, 119, 1720
- Danieli, S., van Dokkum, P., Merritt, A., et al. 2017, *ApJ*, 837, 136
- Dolphin, A.E. 2002, *MNRAS*, 332, 91
- Glasebrook, K., & Bland-Hawthorn, J. 2001, *PASP*, 113, 107
- Haynes, M.P., & Giovanelli, R. 1986, *ApJL*, 306, L55
- Javanmardi, B., & Kroupa, P. 2020, arXiv:2001.02680
- Kaisin, S.S., & Karachentsev, I.D. 2013, *AstrBu*, 68, 381
- Karachentsev, I.D., & Makarova, L.N. 2019, *Astrophysics*, 62, 293
- Karachentsev, I.D., & Karachentseva, V.E. 2019, *MNRAS*, 486, 3697
- Karachentsev, I.D., Makarov, D.I., & Kaisina, E.I. 2013, *AJ*, 145, 101
- Karachentsev, I. D. Makarov, D.I., Sharina, M.E., et al. 2003, *A&A*, 398, 479
- Karachentsev, I.D., Karachentseva, V.E., & Huchtmeier, W.K. 2001, *A&A*, 366, 428
- Makarov, D., Makarova, L., Rizzi, L., et al. 2006, *AJ*, 132, 2729
- Rizzi, L., Tully, R.B., Makarov, D., et al. 2007, *ApJ*, 661, 815
- Ruiz, P., Trujillo, I., & Marmol-Queralto, E. 2015, *MNRAS*, 454, 1605
- Saha, A., Claver, J., & Hoessel, J.G. 2002, *AJ*, 124, 839
- Sand, D.J., Crnoevic, D., Strader, J., et al. 2014, *ApJ*, 793L, 7
- Schlafly, E.F., & Finkbeiner, D.P. 2011, *ApJ*, 737, 103
- Toloba, E., Sand, D.J., Spekkens, K., et al. 2016, *ApJ*, 816, L5
- Tully, R.B., Pomarède, D., Graziani, R., et al. 2019, *ApJ*, 880, 24

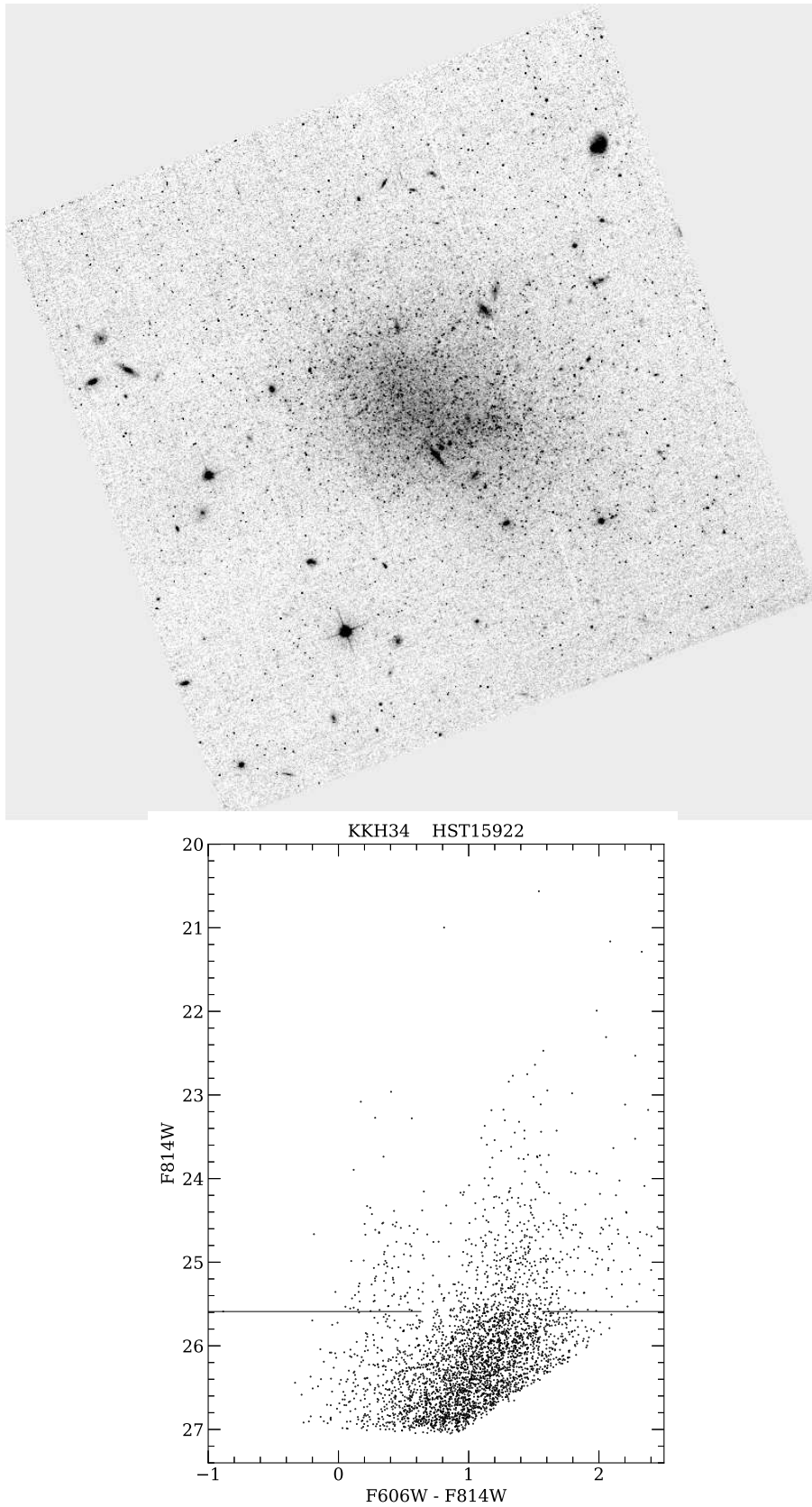


Fig. 6. ACS F814W-filter image of 1.5 x 1.5 arcmin (upper panel) and CM diagram (lower panel) for the dwarf irregular galaxy KKH 34.